

This document is the Accepted Manuscript version of a Published Work that appeared in final form in The Journal of Molecular Spectroscopy, copyright © Elsevier Inc., under the citation mentioned below:

Investigation of the rotamers of 3-furfural by microwave spectroscopy © 2020 by Carolyn Gregory, Jennifer van Wijngaarden is licensed under CC BY-NC-ND 4.0

DOI: <https://doi.org/10.1016/j.jms.2020.111374>

## **Investigation of the Rotamers of 3-Furfural by Microwave Spectroscopy**

Carolyn Gregory and Jennifer van Wijngaarden\*

Department of Chemistry, University of Manitoba, Winnipeg, Manitoba, R3T 2N2, Canada

\*Corresponding author

Email: [vanwijng@cc.umanitoba.ca](mailto:vanwijng@cc.umanitoba.ca)

Phone: (204)474-8379

Fax: (204)474-7608

## Abstract

The rotational spectrum of 3-furfural (3-FF) was investigated using Fourier transform microwave spectroscopy from 6 to 19 GHz in order to examine the rotational isomerism properties of the formyl group relative to the furan ring backbone. Two planar rotamers with the formyl group *anti* or *syn* to the ring oxygen atom were observed with the latter being identified in the gas phase for the first time. The observed relative intensity of  $\sim 8:1$  (*anti:syn*) of transitions is consistent with quantum chemical calculations at the B3LYP-D3(BJ)/aug-cc-pVTZ level which predict that the *anti* rotamer is more stable than the *syn* by 4.86 kJ/mol. Transitions due to singly-substituted  $^{13}\text{C}$  isotopologues for both rotamers and the  $^{18}\text{O}$  isotopologues for the *anti* form were assigned. The resulting sets of rotational constants allowed derivation of accurate ground state effective ( $r_0$ ) and mass dependent ( $r_m^{(1)}$ ) geometries for the furan ring of each rotamer for comparison with their equilibrium ( $r_e$ ) geometries. The *syn/anti* arrangement of the formyl group appears to have little effect on the geometry of the furan ring itself but the exocyclic group is rotated slightly closer to the oxygen atom of the heterocycle when in the *anti* arrangement.

## **Introduction**

Furan derivatives are of broad scientific interest as important degradation products of carbohydrates including simple sugars such as ribose. Furfurals (or furaldehydes), which contain a formyl substituent ( $-(C=O)H$ ) on the furan ( $C_4H_4O$ ) backbone, are considered to be one of the top value-added chemicals [1] derived from woody biomass as they can be converted in one or two synthetic steps to industrially relevant solvents such as furfuryl alcohol, tetrahydrofuran and maleic anhydride [2] or used directly, for example, as building blocks in the plastics industry [3] or as constituents of additives in fracking [4]. As by-products of the breakdown of biomass, furfurals are also known trace constituents of natural environments ranging from forest fires [5], to the microbiome of skin [6] to honey [7].

Beyond the far ranging applications of furfurals, their chemical and physical properties are also of academic interest as prototypical examples of rotational isomerization which is depicted in Figure 1 for 3-furfural (3-FF), the subject of this study. The *anti* rotamer has the carbonyl oxygen atom directed away from the oxygen of the furan ring and rotation about the C3-C6 bond by  $180^\circ$  gives the *syn* rotamer. Its structural isomer, 2-furfural (2-FF), has been well-characterized by various spectroscopic techniques including gas phase rotational [8–10] and vibrational [11,12] spectroscopy. Analysis of its far infrared spectrum of the out-of-plane torsion of the formyl group at  $146.25\text{ cm}^{-1}$  and its hot bands allowed derivation of the underlying asymmetric torsion potential. This provided experimental confirmation, free of solvent effects, that the *anti* rotamer is  $3.42(29)$  kJ/mol lower in energy than its *syn* counterpart and that the barrier to rotational isomerization is  $38.94(6)$  kJ/mol. The high barrier, which prevents facile interconversion to the lower energy form, allowed both rotamers to be observed via Fourier transform microwave (FTMW) spectroscopy in a cold supersonic jet [10]. For 3-FF, in contrast, comparable details regarding the relationship

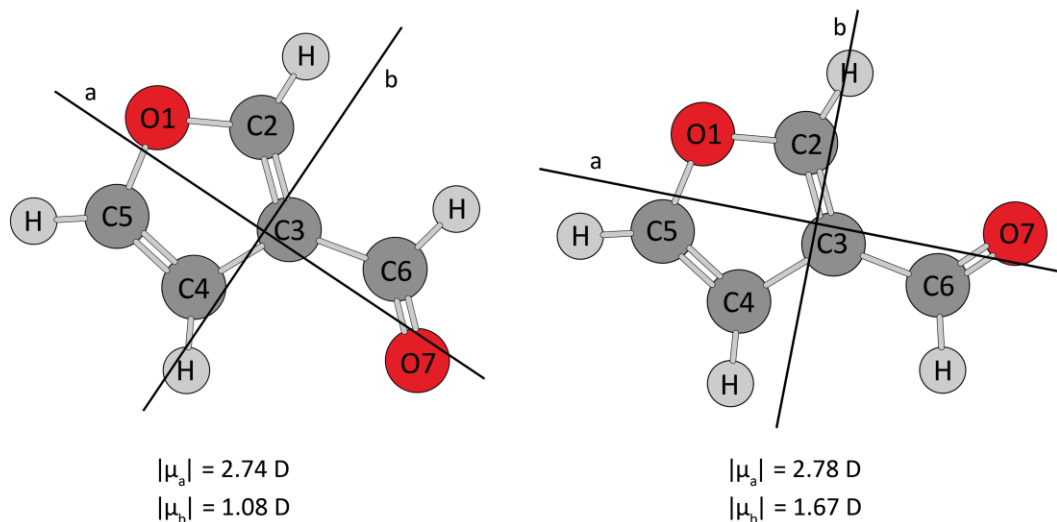


**Figure 1.** Principal axes and dipole moments for the *anti* (left) and *syn* (right) conformers of 3-FF. Dipole moments (Debye) were calculated at the B3LYP-D3(BJ)/aug-cc-pVTZ level of theory.

between the rotational isomers are not available as only the *anti* rotamer has been observed in previous gas phase rotational [13] and vibrational [13][14] studies. Solution NMR studies have established that the *syn* rotamer is present in small amounts (2-6%) in various solvents [15] at room temperature with estimates of its relative abundance reaching as much as 14( $\pm$ 3)% from Nuclear Overhauser Effect (NOE) studies [16]. This is remarkably similar to the value derived from an infrared study of 3-FF seeded in Ar matrices which estimated that the proportion of the *anti:syn* rotamers in the gas phase is 7:1 (or 14% *syn*) at room temperature [17] and is supported by quantum chemical estimates at the B3LYP/6-311++G(d,p) level which place the *anti* rotamer 4.03 kJ/mol lower in energy [17]. From NMR line shape analysis, the barrier to isomerization was estimated to be 34.7 kJ/mol [16] which is also inline with the computational prediction of 34.4 kJ/mol for the *anti* to *syn* conversion pathway [17].

Based on the above, it is somewhat surprising that the *syn* conformer of 3-FF has not been previously observed via microwave spectroscopy as a similar energy landscape in 2-FF did not preclude observation of the higher energy rotamer. Using a Stark-modulated microwave spectrometer, Marstokk and Møllendal [13] assigned rotational transitions for the *anti* rotamer of 3-FF and several excited torsional states at -15°C but were unsuccessful in assigning features to the *syn* rotamer despite a careful search guided by quantum chemical calculations. The absence of a spectrum from the higher energy rotamer, in fact, led them to conclude that it must lie more than 5 kJ/mol higher in energy than the *anti* form which would imply that the true barrier is at least 20% higher than previously estimated from condensed phase experiments.

This discrepancy led us to investigate 3-FF using a combination of FTMW spectroscopy and quantum chemical calculations at the B3LYP-D3(BJ)/aug-cc-pVTZ level of theory. In this paper, we present the first rotational spectrum of the *syn* rotamer of 3-FF which is confirmed by analysis of transitions due to its five <sup>13</sup>C isotopologues in natural abundance. We also report herein the first rotational spectrum of the five <sup>13</sup>C and two <sup>18</sup>O isotopologues of the dominant *anti* rotamer. The accurate rotational constants derived for both *syn*- and *anti*-3-FF were used to determine experimental ground state geometries for comparison with the equilibrium geometry and to investigate whether the orientation of the formyl substituent alters the geometry of the furan backbone.

## **Experimental**

3-FF (98%), a liquid at room temperature (bp 144°C), was purchased from ACROS Organics and used without further purification. The sample was added to a glass bubbler and the neon carrier gas with a pressure of ~1 bar was seeded with 3-FF vapour from the room temperature

sample. The resulting gas mixture was introduced into the high vacuum chambers of the instruments through a pulsed nozzle to create a supersonic jet in which molecules are typically at rotational temperatures below 5 K. The FTMW spectrum was subsequently collected using both the chirped pulse (cp) and Balle-Flygare spectrometers which have been described previously [18,19]. The former was used to rapidly record a survey spectrum from 9-17 GHz in segments of 2 GHz from which transitions corresponding to the two conformers and their singly substituted isotopologues were preliminarily assigned. Individual transitions were then collected using the higher resolution Balle-Flygare instrument in the range of 6-19 GHz to determine more precise line centres and to record additional, lower intensity features. Spectra recorded with the cavity-based instrument have linewidths (FWHM) of  $\sim 7$  kHz and individual frequencies are typically measured to within  $\pm 1$  kHz.

### **Computational Details**

Quantum chemical calculations for both *anti* and *syn* conformers of 3-FF were conducted using Gaussian 16 software [20]. Geometry optimizations were calculated at the B3LYP-D3(BJ)/aug-cc-pVTZ level of theory and the resulting equilibrium structures in their principal inertial axis systems are given in Figure 1. These geometries were verified to be true minima on the potential energy surface using harmonic frequency calculations. The internal coordinates for both rotamers are provided in the SI. The conversion barrier between the rotamers was estimated by performing an energy scan of the C2-C3-C6-O7 dihedral angle at the same level of theory with a step size of  $10^\circ$  from the *anti* to the *syn* geometry, with all other geometric parameters relaxed. The resulting energy profile is shown in Figure 2.

## Results

### I. Spectral Fitting

The energy difference between the *anti* and *syn* rotamers of 3-FF is estimated to be 4.86 kJ/mol (B3LYP-D3(BJ)/aug-cc-pVTZ) and hence the relative population of the *syn* species is expected to be ~12.3% at room temperature based on the Boltzmann equation. The barrier to internal rotation of the formyl group is 34.3 kJ/mol (Figure 2) from the higher energy rotamer which indicates that the *syn* form is metastable as the barrier is well above that (~4.8 kJ/mol) derived from empirical studies of relaxation in supersonic jets [21]. Based on the calculated electric dipole components, summarized in Figure 1, the rotational spectrum of 3-FF should consist of both *a*- and *b*-type transitions of the two rotamers.

A portion of the survey spectrum recorded with the cp-FTMW instrument is shown in Figure 3 and is dominated by transitions from the *anti* rotamer as expected but lower intensity transitions consistent with the *syn* form are also visible. From this spectrum, we were also able to

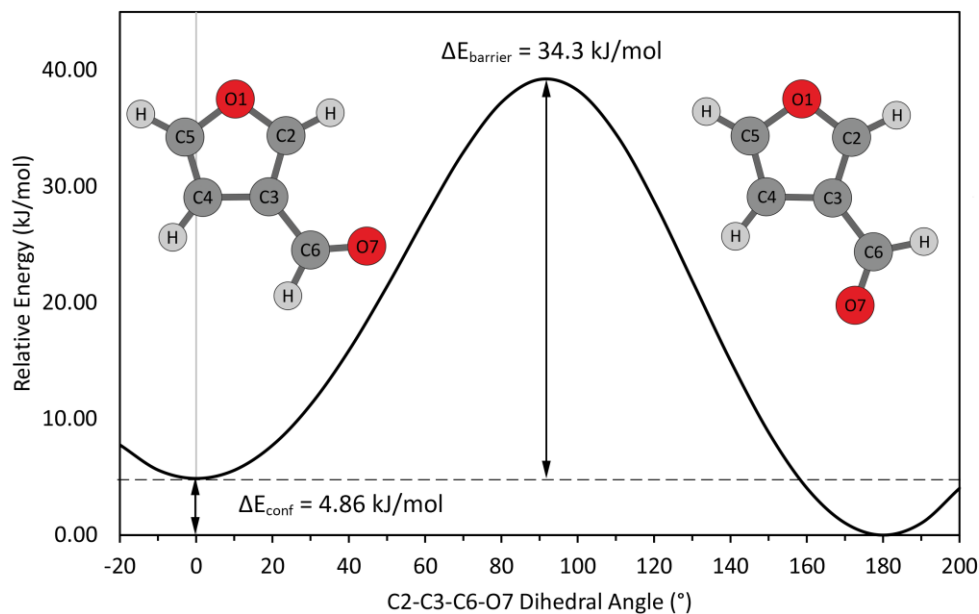


**Figure 2.** Calculated barrier (B3LYP-D3(BJ)/aug-cc-pVTZ) for the torsion about the formyl substitution between *syn*- and *anti*-3-furfural.

identify features due to the five singly substituted  $^{13}\text{C}$  and two  $^{18}\text{O}$  isotopologues of *anti*-3-FF and the five  $^{13}\text{C}$  species of *syn*-3-FF in natural abundance. The assigned transitions of each isotopologue were fit using Pickett's SPFIT program (Watson's A-reduced Hamiltonian  $I'$  representation) [22] and the spectroscopic constants determined are given in Tables 1 and 2. As fewer transitions were observed for the minor isotopologues of the two rotamers, some centrifugal distortion constants were not well-determined from the fit and were subsequently fixed to the parent values. The rms errors of the fits were below 1.2 kHz which indicated that the model Hamiltonian provides a good description of the energy levels sampled in the observed rotational spectra.

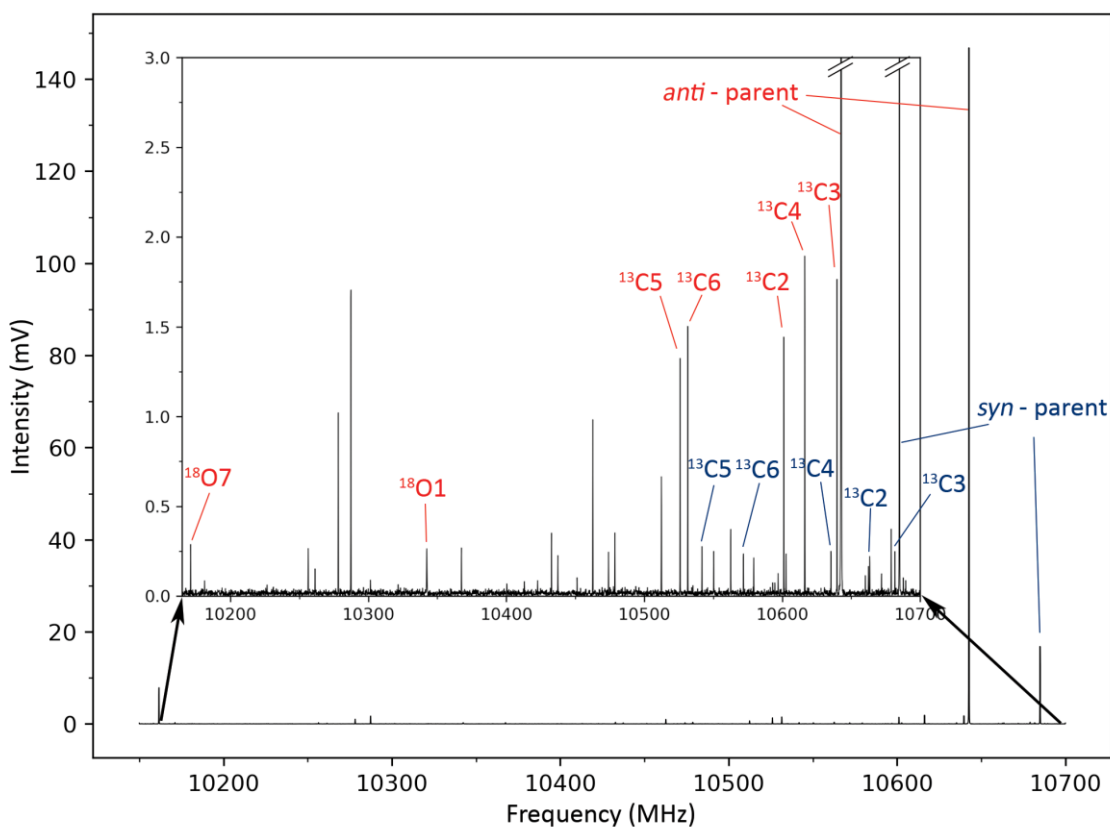


**Figure 3.** Portion of the cp-FTMW spectrum (500 000 FIDs averaged) of 3-furfural showing the relative intensity of the  $J K_a K_c: 3_{03}-2_{02}$  transition for the parent, five  $^{13}\text{C}$  isotopologues and two  $^{18}\text{O}$  isotopologues of the *anti* rotamer (red) and the parent and five  $^{13}\text{C}$  isotopologues for the *syn* rotamer (blue). The inset is a magnification of the bottom trace.



**Table 1.** Ground state spectroscopic constants of *anti*-3-furfural and its  $^{13}\text{C}$  and  $^{18}\text{O}$  isotopologues.

	Parent	$^{18}\text{O}1$	$^{13}\text{C}2$	$^{13}\text{C}3$	$^{13}\text{C}4$	$^{13}\text{C}5$	$^{13}\text{C}6$	$^{18}\text{O}7$
Rotational Constants <sup>a</sup> /MHz								
A	8238.73071(13)	8182.7750(3)	8081.66955(26)	8234.31652(22)	8077.7283(3)	8139.1877(3)	8205.70856(20)	8211.00876(16)
B	1976.13983(3)	1920.71738(11)	1972.01052(13)	1975.64226(5)	1975.29373(19)	1954.73513(12)	1954.01772(13)	1879.58529(7)
C	1593.97178(3)	1555.70967(8)	1585.32427(10)	1593.48872(7)	1587.29767(18)	1576.31539(11)	1578.33372(10)	1529.59162(5)
Centrifugal Distortion Constants/kHz								
$\Delta_J$	0.1401(6)	0.1256(15)	0.1301(19)	0.1381(6)	0.1391(22)	0.1395(17)	0.1332(18)	0.1329(10)
$\Delta_{JK}$	0.7319(22)	0.737(6)	0.757(8)	0.724(4)	0.761(11)	0.667(8)	[0.7319]	0.665(3)
$\Delta_K$	1.79(3)	[1.79]	[1.79]	1.86(5)	1.48(9)	1.69(8)	[1.79]	[1.79]
$\delta_J$	0.03071(10)	0.0270(10)	0.0255(12)	0.0308(3)	0.0285(5)	0.0305(6)	0.0258(12)	0.0299(6)
$\delta_K$	0.837(11)	[0.837]	[0.837]	0.778(24)	0.95(8)	0.86(3)	[0.837]	[0.837]
# lines	51	35	36	42	37	41	34	36
rms	0.33	0.84	1.06	0.49	0.73	0.83	1.04	0.57

<sup>a</sup>Calculated rotational constants (B3LYP-D3(BJ)/aug-cc-pVTZ) for *anti*-3FF: A = 8282.4 MHz, B = 1983.0 MHz, C = 1599.9 MHz.

Rotational constants from ref [13]: A = 8238.7276(16) MHz, B = 1976.13883(42) MHz, C = 1593.97114(34) MHz. <sup>b</sup>Calculated centrifugal distortion constants (B3LYP-D3(BJ)/aug-cc-pVTZ):  $\Delta_J$  = 0.1340 kHz,  $\Delta_{JK}$  = 0.5615 kHz,  $\Delta_K$  = 2.005 kHz,  $\delta_J$  = 0.03049 kHz,  $\delta_K$  = 0.7650 kHz.

**Table 2.** Ground state spectroscopic constants of *syn*-3-furfural and its  $^{13}\text{C}$  isotopologues.

	Parent	$^{13}\text{C}2$	$^{13}\text{C}3$	$^{13}\text{C}4$	$^{13}\text{C}5$	$^{13}\text{C}6$
Rotational Constants <sup>a</sup> /MHz						
A	8158.58900(12)	8031.6972(4)	8151.5264(3)	7976.10251(25)	8130.1998(3)	8126.1532(6)
B	1987.10519(3)	1986.38489(13)	1986.63690(8)	1982.20042(15)	1958.16499(11)	1964.51579(18)
C	1598.20367(3)	1592.80768(10)	1597.63463(7)	1587.91588(11)	1578.36593(8)	1582.33814(14)
Centrifugal Distortion Constants/kHz						
$\Delta_J$	0.1489(4)	0.1478(16)	0.1471(15)	0.1393(20)	0.1408(18)	0.1414(25)
$\Delta_{JK}$	0.595(3)	0.653(12)	0.581(11)	[0.595]	[0.595]	0.559(14)
$\Delta_K$	1.901(9)	[1.901]	[1.901]	[1.901]	[1.901]	[1.901]
$\delta_J$	0.03376(10)	0.0302(16)	0.0338(4)	0.0284(21)	0.0312(6)	0.0327(17)
$\delta_K$	0.826(5)	[0.826]	[0.826]	[0.826]	[0.826]	[0.826]
# lines	56	22	28	27	26	25
rms	0.54	0.67	0.64	1.02	0.84	1.19

<sup>a</sup>Calculated rotational constants (B3LYP-D3(BJ)/aug-cc-pVTZ) for *syn*-3FF: A = 8223.0 MHz, B = 1990.9 MHz, C = 1602.8 MHz. <sup>b</sup>Calculated centrifugal distortion constants (B3LYP-D3(BJ)/aug-cc-pVTZ):  $\Delta_J$  = 0.1396 kHz,  $\Delta_{JK}$  = 0.6123 kHz,  $\Delta_K$  = 1.808 kHz,  $\delta_J$  = 0.03166 kHz,  $\delta_K$  = 0.7882 kHz.

## II. Structural Determination

Both the *anti* and *syn* rotamers have small inertial defects ( $\Delta$ ) of  $-0.0259 \text{ amu}\cdot\text{\AA}^2$  and  $-0.0568 \text{ amu}\cdot\text{\AA}^2$ , respectively as expected for planar molecules. Negative values of  $\Delta$  are commonly attributed to contributions from low frequency out-of-plane motions [23]. As rotational transitions were observed for a large number of isotopologues, eight for *anti* and six for *syn*, the geometries of the heavy atom backbones of *anti* and *syn*-3-FF were estimated by various approaches as described below.

The Kraitchman [24] substitution  $r_s$  structures of both conformers were derived using Kisiel's KRA program [25] with the relative signs of the coordinates determined by comparison to the DFT results. The  $r_s$  coordinates for both rotamers are given in the supplemental data. The Kraitchman coordinates and Costain errors [26] were then used in conjunction with the EVAL routine [25] to derive internal parameters for the heavy atoms of the *anti* rotamer and for the carbon backbone of the *syn* conformer. As the ground state of 3-FF is effectively planar, some of the  $c$ -coordinates of each rotamer were imaginary and even if set to zero, the geometric parameters derived from the  $a$ - and  $b$ -coordinates did not provide good agreement with the  $r_e$  parameters determined at the B3LYP/aug-cc-pVTZ level of theory. A similar issue occurred in the derivation of the  $r_s$  geometry of 2-FF [12] and was attributed to the two things: i) the comparatively large Costain errors associated with atoms lying close to inertial axes and ii) the untreated vibrational effects arising from low energy torsion of the formyl group. As Figure 1 shows, both rotamers of 3-FF similarly have atoms close to the  $a$ - and  $b$ -axes and computational estimates (B3LYP/6-311++G(d,p))[17] suggest that the formyl torsion is even lower frequency ( $130\text{-}134 \text{ cm}^{-1}$ ) [17] than that of 2-FF (expt:  $146.25 \text{ cm}^{-1}$ )[12].

An alternative approach is to perform a least squares fit of select internal coordinates of 3-

FF to the moments of inertia taken from the rotational constants in Tables 1 and 2 to derive the ground state effective  $r_0$  geometries as implemented in Kisiel's STRFIT program [25]. Without data for deuterium isotopes to work with, the hydrogen atom coordinates were fixed to their equilibrium values calculated at the B3LYP-D3(BJ)/aug-cc-pVTZ level. With additional data derived from the  $^{18}\text{O}$  isotopologues of the *anti* rotamer, this procedure worked reasonably well when all 24 rotational constants (A, B, C for all isotopologues) were included. For the *syn* form, for which only  $^{13}\text{C}$  isotopic data was available, the uncertainties in the derived geometric parameters were quite large (up to 0.04 Å in bond lengths). As both rotamers have planar equilibrium structures, there are theoretically only two independent moments of inertia for each isotopologue and when we repeated the fitting routine using only A and B rotational constants, a satisfactory fit in which moments of inertia were determined to within 0.015% ( $I_{\text{obs}} - I_{\text{calc}}/I_{\text{obs}}$ ) was

**Table 3.** Equilibrium ( $r_e$ ) (B3LYP-D3(BJ)/aug-cc-pVTZ), ground state ( $r_0$ ), and ground state mass dependent ( $r_m^{(1)}$ ) structural parameters (bond lengths in Å, angles in degrees) determined for *anti*- and *syn*-3-furfural.

	<i>anti</i> -3-FF			<i>syn</i> -3-FF		
	$r_e$	$r_0^a$	$r_m^{(1)b}$	$r_e$	$r_0^a$	$r_m^{(1)b}$
O1-C2	1.347	1.356(3)	1.355(3)	1.347	1.343(14)	1.340(9)
C2-C3	1.365	1.368(4)	1.367(3)	1.366	1.366(7)	1.363(5)
C3-C4	1.438	1.446(3)	1.441(2)	1.438	1.443(7)	1.443(5)
C4-C5	1.349	1.353(4)	1.352(3)	1.351	1.356(6)	1.355(4)
C5-O1	1.374	1.377(3)	1.376(2)	1.371	1.375(7)	1.373(5)
C3-C6	1.458	1.457(3)	1.458(3)	1.460	1.469(7)	1.469(5)
C6-O7	1.211	1.217(3)	1.213(2)	1.211	1.218(7)	1.215(4)
$\angle(\text{O1-C2-C3})$	110.6	110.9(2)	110.7(2)	110.3	110.7(5)	110.8(3)
$\angle(\text{C2-C3-C4})$	105.9	105.7(3)	105.9(2)	105.9	105.9(6)	105.9(4)
$\angle(\text{C3-C4-C5})$	106.1	106.1(2)	106.1(1)	106.3	105.9(3)	105.8(2)
$\angle(\text{C4-C5-O1})$	110.5	110.7(1)	110.7(1)	110.1	110.2(5)	110.2(3)
$\angle(\text{C5-O1-C2})$	106.9	106.7(1)	106.6(1)	107.4	107.3(5)	107.4(3)
$\angle(\text{C2-C3-C6})$	125.7	125.9(2)	125.8(2)	126.7	126.7(6)	126.7(4)
$\angle(\text{C4-C3-C6})$	128.4	128.4(2)	128.3(2)	127.4	127.4(4)	127.4(3)
$\angle(\text{C3-C6-O7})$	124.5	123.7(2)	123.9(2)	124.8	123.9(5)	124.1(3)
$\sigma_{\text{fit}} (\text{u } \text{Å}^2)$		0.0051	0.0053		0.0070	0.0059

<sup>a</sup> Ground state ( $r_0$ ) geometries were derived using A and B constants only.

<sup>b</sup> Additional  $r_m^{(1)}$  parameter ( $c_a = c_b = c_c$ ) for *anti*-3-FF: 0.0043(5)  $\text{u}^{1/2}$  Å; for *syn*-3-FF: 0.0094(7)  $\text{u}^{1/2}$  Å.

obtained for both *syn*- and *anti*-3-FF. The resulting  $r_0$  parameters are summarized in Table 3 along with the  $r_e$  values for comparison.

An improved structural estimate of both *syn*- and *anti*-3-FF was obtained using Watson's mass dependence method to derive  $r_m^{(1)}$  parameters [27]. This allowed the inclusion of all three rotational constants for the parent and each isotopic species in the fits in Kisiel's STRFIT program [25] with the Laurie parameter  $\delta_H$  fixed to 0.01 Å for each CH bond. The approximation that the mass dependence parameters associated with the inertial axes were equal (i.e.  $c_a=c_b=c_c$ ) was also used to reduce the number of parameters in the fits as was reported previously for the planar benzaldehyde [28] and fluorobenzaldehyde [29] rings. Using this method, the moments of inertia were reproduced to within 0.007%. The derived  $r_m^{(1)}$  parameters are given in Table 3.

## **Discussion**

The rotational and centrifugal distortion constants of both rotamers were well-determined and in agreement with DFT estimates as shown in Tables 1 and 2. For *anti*-3-FF, the high resolution of the FTMW instrument allowed for a more precise determination of the spectroscopic parameters of the parent compound as compared to the previous MW absorption study [13] where line positions were reported with less precision ( $\pm 0.05$  MHz). The current study also enabled identification of transitions due to its  $^{13}\text{C}$  and  $^{18}\text{O}$  isotopologues for the first time. The rotational spectrum of the *syn* rotamer, which was previously assumed to be too high in energy to be sufficiently populated, was observed here for the first time with spectral intensities approximately 1/8 that of the dominant *anti* rotamer when comparing transitions close in frequency with the same quantum numbers. As the *a*-axis dipole components of the *anti* and *syn* species are nearly identical (Figure 1), this suggests that the latter has a relative abundance of ~12.5% (based on the spectral

intensities) in the jet and lies 4.83 kJ/mol higher in energy. This is supported by our quantum chemical predictions of the relative energy difference of 4.86 kJ/mol (B3LYP-D3(BJ)/aug-cc-pVTZ) (Figure 2). It is unclear why Marstokk and Møllendal [13] were unable to detect the *syn* rotamer as they successfully assigned rotational transitions in the 4<sup>th</sup> excited torsional state of the *anti* rotamer which lies at  $\sim 520\text{ cm}^{-1}$  (6.2 kJ/mol) based on our harmonic frequency calculations. We note that the quantum chemical predictions for the rotational constants of the *syn* rotamer in Table 2 (and those reported in Ref [13] at the MP2/6-31(d) level) reveal a greater discrepancy with the experimental constants than in the case of the *anti* rotamer in Table 1. We believe that the failure to identify the *syn*-3-FF spectrum earlier was most likely that the transition frequencies were outside the search range rather than a result of insufficient population. Using the broadband capabilities of a modern chirped-pulse FTMW spectrometer in the present study, it was straightforward to identify the spectral features *syn*-3-FF.

The experimental  $r_0$  and  $r_m^{(1)}$  geometries determined for the two rotamers of 3-FF are given in Table 3. A comparison of the values reveals that the two methods yield very similar results with the biggest difference seen for the *syn* rotamer which had a smaller set of isotopologues to work with. In this case, the inclusion of additional parameters ( $c_\alpha$ ,  $\delta_H$ ) in the  $r_m^{(1)}$  fit served to reduce the standard deviation in the derived bond lengths and angles. This may simply be the result of an extra variable ( $c_\alpha$ ) although this method allowed the use of all three rotational constants for each isotopologue which is meant to correct for contributions from low frequency modes such as the formyl torsion. In comparing the experimentally derived structures with the quantum chemical estimates ( $r_e$ ) in Table 3, the agreement is good overall with most parameters matching the calculated values to within 1-2  $\sigma$ .

Comparing the equilibrium geometries of the *syn*- and *anti*-3-FF rotamers in Table 3, the furan backbone appears largely unaffected by the *syn/anti* arrangement of the formyl group suggesting that there is no substantial perturbative interaction between the C=O group and the ring through the  $\pi$  bonding orbitals or the lone pairs on the carbonyl oxygen. A similar result was reported in benzaldehyde where the bond lengths in the benzene backbone were not dependent on the position of the C=O bond [28]. For 3-FF, the main geometric difference appears in the orientation of the C3-C6 bond of the formyl group relative to the ring. In the *anti* case, the angle of the substituent brings it  $\sim 2.7^\circ$  closer to the C2-C3 bond as seen through the introduction of a small asymmetry in the  $\angle C4-C3-C6$  and  $\angle C2-C3-C6$  angles whereas these angles are the same to within  $0.7^\circ$  in the *syn* rotamer. This points to subtle differences in the interaction between the formyl substituent with the furan ring for the two rotamers. In the structural isomer 2-FF, the orientation of the formyl group is also affected by  $\sim 2^\circ$  in comparing the geometries of *syn* versus *anti*-2-FF [10]. In the *syn* rotamer of 2-FF, the C=O bond is rotated further away from the oxygen of the furan ring presumably to minimize repulsive interactions between the two electronegative oxygen atoms in close proximity. We suspect that this is not the driving force in 3-FF because the groups are too far apart as the O...O distances are 4.270 Å and 4.587 Å in the *syn* and *anti* rotamers, respectively based on the  $r_e$  geometries. From a natural bond orbital (NBO) analysis, Kuş *et al.* [17] used natural charges to suggest that the *anti* rotamer is stabilized relative to its *syn* counterpart by a more attractive dipolar interaction between C4-H and C6=O which would favour the formyl group adopting a slightly larger C2-C3-C6 angle in the *syn* versus *anti* rotamer as seen here. From the NBO results presented in reference [17], we feel the best explanation for this geometric difference is the stabilizing  $\pi(C2-C3) \rightarrow \pi^*(C6=O)$  interaction which is estimated to be

5 kJ/mol stronger in *anti*-3-FF than *syn*-3-FF and would favour a slightly smaller  $\angle$ C2-C3-C6 angle in the former.

## Conclusions

The rotational spectra of the two planar rotamers of 3-FF and their heavy atom analogues have been recorded and analysed to derive accurate experimental geometries using both  $r_0$  and  $r_m^{(1)}$  methods. The results compare favourably with the B3LYP-D3(BJ)/aug-cc-pVTZ equilibrium  $r_e$  structure and suggest that the orientation of the formyl group has little effect on the geometry of the furan ring backbone as most bond lengths and angles of *anti*-3-FF and *syn*-3-FF match to within the derived experimental uncertainties. As in its structural isomer 2-FF, the largest change occurs in the orientation of the formyl group relative to the ring. In *anti*-3-FF, the exocyclic substituent is rotated slightly closer to the C2-C3 bond which is likely due to stabilization from an interaction of type:  $\pi(\text{C2-C3}) \rightarrow \pi^*(\text{C6=O})$ . This may also explain why the *anti*-3-FF form is lower in energy by nearly 5 kJ/mol as there is no comparable  $\pi$  bond associated with the C3-C4 bond to stabilize the *syn* rotamer.

## Supporting Information

Appendix I: Equilibrium (B3LYP-D3(BJ)/aug-cc-pVTZ) and literature ground state spectroscopic constants

Appendix II: Equilibrium Structures from B3LYP-D3(BJ)/aug-cc-pVTZ

Appendix III: Assigned Transitions for 3-furfural

Appendix IV: Kraitchman Coordinates ( $r_s$ )

## **Acknowledgements**

This research is funded by the Natural Sciences and Engineering Research Council of Canada (NSERC) through the Discovery Grant program. CG is grateful for financial support provided through the SEGS program from the Faculty of Science at the University of Manitoba.

## **References**

- [1] R. Mariscal, P. Maireles-Torres, M. Ojeda, I. Sádaba, M. López Granados, Furfural: A renewable and versatile platform molecule for the synthesis of chemicals and fuels, *Energy Environ. Sci.* 9 (2016) 1144–1189. <https://doi.org/10.1039/c5ee02666k>.
- [2] K. Dalvand, J. Rubin, S. Gunukula, M. Clayton Wheeler, G. Hunt, Economics of biofuels: Market potential of furfural and its derivatives, *Biomass and Bioenergy.* 115 (2018) 56–63. <https://doi.org/10.1016/j.biombioe.2018.04.005>.
- [3] Y. Tachibana, S. Kimura, K.I. Kasuya, Synthesis and Verification of Biobased Terephthalic Acid from Furfural, *Sci. Rep.* 5 (2015) 8249 (1–5). <https://doi.org/10.1038/srep08249>.
- [4] K.E. Manz, T.J. Adams, K.E. Carter, Furfural degradation through heat-activated persulfate: Impacts of simulated brine and elevated pressures, *Chem. Eng. J.* 353 (2018) 727–735. <https://doi.org/10.1016/j.cej.2018.07.142>.
- [5] T.G. Karl, T.J. Christian, R.J. Yokelson, P. Artaxo, W.M. Hao, A. Guenther, The Tropical Forest and Fire Emissions Experiment: method evaluation of volatile organic compound emissions measured by PTR-MS, FTIR, and GC from tropical biomass burning, *Atmos. Chem. Phys.* 7 (2007) 5883–5897. <https://doi.org/10.5194/acp-7-5883-2007>.
- [6] S. Ron-Doitch, Y. Soroka, M. Frusic-Zlotkin, D. Barasch, D. Steinberg, R. Kohen, Saturated and aromatic aldehydes originating from skin and cutaneous bacteria activate the Nrf2-keap1 pathway in human keratinocytes, *Exp. Dermatol.* 00 (2020) 1-7. <https://doi.org/10.1111/exd.14103>.
- [7] Y. Yang, M.-J. Battesti, J. Costa, N. Dupuy, J. Paolini, Volatile components as chemical markers



- of the botanical origin of Corsican honeys, *Flavour Fragr. J.* 33 (2018) 52–62.  
<https://doi.org/10.1002/ffj.3414>.
- [8] F. Mönnig, H. Dreizler, H.D. Rudolph, Mikrowellenspektrum von furfurol und thiophen-2-aldehyd, *Z. Naturforsch.* 20a (1965) 1323–1326. <https://doi.org/10.1515/zna-1965-1015>.
- [9] F. Mönnig, H. Dreizler, H.D. Rudolph, Rotationsspektren in angeregten Schwingungszuständen und Torsionspotential von Furfurol, *Z. Naturforsch.* 21a (1966) 1633–164.  
<https://doi.org/10.1515/zna-1966-1013>.
- [10] R.A. Motiyenko, E.A. Alekseev, S.F. Dyubko, F.J. Lovas, Microwave spectrum and structure of furfural, *J. Mol. Spectrosc.* 240 (2006) 93–101. <https://doi.org/10.1016/j.jms.2006.09.003>.
- [11] F.A. Miller, W.G. Fateley, R.E. Witkowski, Torsional frequencies in the far infrared- V. Torsions around the C-C single bond in some benzaldehydes, furfural, and related compounds, *Spectrochim. Acta.* 23A (1967) 891–908. [https://doi.org/10.1016/0584-8539\(67\)80016-3](https://doi.org/10.1016/0584-8539(67)80016-3).
- [12] T.S. Little, J. Qiu, J.R. Durig, Asymmetric torsional potential function and conformational analysis of furfural by far infrared and Raman spectroscopy, *Spectrochim. Acta.* 45A (1989) 789–794. [https://doi.org/10.1016/0584-8539\(89\)80215-6](https://doi.org/10.1016/0584-8539(89)80215-6).
- [13] K.-M. Marstokk, H. Møllendal, Microwave Spectrum, Conformation and Dipole Moment of Furan-3-carboxaldehyde., *Acta Chem. Scand.* 46 (1992) 923–927.  
<https://doi.org/10.3891/acta.chem.scand.46-0923>.
- [14] K. Volka, P. Adámek, I. Stibor, Z. Ksandr, Utilization of stable isotopes for the study of vibrational spectra of furaldehydes, *J. Radioanal. Chemistry.* 30 (1976) 205–214.  
<https://doi.org/10.1007/BF02516631>.
- [15] R. Benassi, U. Folli, A. Mucci, L. Schenetti, F. Taddei, Long-range  $^{13}\text{C}$ - $^1\text{H}$  spin-spin coupling constants in the conformational analysis of formyl derivatives of furan and thiophene, *Magn. Reson. Chem.* 25 (1987) 804–810. <https://doi.org/10.1002/mrc.1260250913>.
- [16] L. Lunazzi, G. Placucci, D. Macciantelli, Stereodynamics and conformation of furan-3-aldehyde and of its corresponding furoyl sigma-radical, *Tetrahedron.* 41 (1991) 6427–6434.

- [https://doi.org/10.1016/S0040-4020\(01\)86570-4](https://doi.org/10.1016/S0040-4020(01)86570-4).
- [17] N. Kuş, I. Reva, R. Fausto, Photoisomerization and photochemistry of matrix-isolated 3-furaldehyde, *J. Phys. Chem. A*. 114 (2010) 12427–12436. <https://doi.org/10.1021/jp1079839>.
- [18] L. Evangelisti, G. Sedo, J. van Wijngaarden, Rotational spectrum of 1,1,1-trifluoro-2-butanone using chirped-pulse Fourier transform microwave spectroscopy, *J. Phys. Chem. A*. 115 (2011) 685-690. <https://doi.org/10.1021/jp1089905>.
- [19] G. Sedo, J. van Wijngaarden, Fourier transform microwave spectra of a new isomer of OCS- CO<sub>2</sub>, *J. Chem. Phys.* 131 (2009) 044303. <https://doi.org/10.1063/1.3186756>.
- [20] M.J. Frisch, G.W. Trucks, H.B. Schlegel, G.E. Scuseria, M.A. Robb, J.R. Cheeseman, G. Scalmani, V. Barone, G.A. Petersson, H. Nakatsuji, X. Li, M. Caricato, A. V. Marenich, J. Bloino, B.G. Janesko, R. Gomperts, B. Mennucci, H.P. Hratchian, J. V. Ortiz, A.F. Izmaylov, J.L. Sonnenberg, D. Williams-Young, F. Ding, F. Lipparini, F. Egidi, J. Goings, B. Peng, A. Petrone, T. Henderson, D. Ranasinghe, V.G. Zakrzewski, J. Gao, N. Rega, G. Zheng, W. Liang, M. Hada, M. Ehara, K. Toyota, R. Fukuda, J. Hasegawa, M. Ishida, T. Nakajima, Y. Honda, O. Kitao, H. Nakai, T. Vreven, K. Throssell, J. Montgomery, J. A., J.E. Peralta, F. Ogliaro, M.J.. Bearpark, J.J. Heyd, E.N. Brothers, K.N. Kudin, V.N. Staroverov, T.A. Keith, R. Kobayashi, J. Normand, K. Raghavachari, A.P. Rendell, J.C. Burant, S.S. Iyengar, J. Tomasi, M. Cossi, J.M. Millam, M. Klene, C. Adamo, R. Cammi, J.W. Ochterski, R.L. Martin, K. Morokuma, O. Farkas, J.B. Foresman, D.J. Fox, Gaussian 16 Revision C.01, (2016).
- [21] R.S. Ruoff, T.D. Klots, T. Emilsson, H.S. Gutowsky, Relaxation of conformers and isomers in seeded supersonic jets of inert gases, *J. Chem. Phys.* 93 (1990) 3142–3150. <https://doi.org/10.1063/1.458848>.
- [22] H.M. Pickett, The fitting and prediction of vibration-rotation spectra with spin interactions, *J. Mol. Spectrosc.* 148 (1991) 371–377. [https://doi.org/10.1016/0022-2852\(91\)90393-O](https://doi.org/10.1016/0022-2852(91)90393-O).
- [23] W. Gordy, R.L. Cooke, *Microwave Molecular Spectra*, 3rd ed., Wiley, New York, 1984.
- [24] J. Kraitchman, Determination of Molecular Structure from Microwave Spectroscopic Data, *Am. J.*

- Phys. 21 (1953) 17–24. <https://doi.org/10.1119/1.1933338>.
- [25] Z. Kisiel, PROSPE - Programs for ROTational SPEctroscopy, (n.d.).  
<http://www.ifpan.edu.pl/~kisiel/prospe.htm> (accessed August 3, 2020).
- [26] C.C. Costain, Further Comments on the Accuracy of rs Substitution Structures, *Trans. Am. Crystallogr. Assoc.* 2 (1966) 157–164.
- [27] J.K.G. Watson, A. Roytburg, W. Ulrich, Least-Squares Mass-Dependence Molecular Structures, *J. Mol. Spectrosc.* 196 (1999) 102–119. <https://doi.org/10.1006/jmsp.1999.7843>.
- [28] O. Desyatnyk, L. Pszczółkowski, S. Thorwirth, T.M. Krygowski, Z. Kisiel, The rotational spectra, electric dipole moments and molecular structures of anisole and benzaldehyde, *Phys. Chem. Chem. Phys.* 7 (2005) 1708–1715. <https://doi.org/10.1039/b501041a>.
- [29] W. Sun, I.B. Lozada, J. Van Wijngaarden, Fourier Transform Microwave Spectroscopic and ab Initio Study of the Rotamers of 2-Fluorobenzaldehyde and 3-Fluorobenzaldehyde, *J. Phys. Chem. A.* 122 (2018) 2060–2068. <https://doi.org/10.1021/acs.jpca.7b11673>.